Depletion of CXCR2 Inhibits Tumor Growth and Angiogenesis in a Murine Model of Lung Cancer[1]

Michael P. Keane,* John A. Belperio,* Ying Y. Xue,* Marie D. Burdick,* and Robert M. Strieter[2]*†

The Glu-Leu-Arg$^+$ (ELR$^+$) CXC chemokines are potent promoters of angiogenesis and have been demonstrated to induce a significant portion of nonsmall cell lung cancer-derived angiogenic activity and support tumorigenesis. ELR$^+$ CXC chemokines share a common chemokine receptor, CXCR2. We hypothesized that CXCR2 mediates the proangiogenic effects of ELR$^+$ CXC chemokines during tumorigenesis. To test this postulate, we used syngeneic murine Lewis lung cancer (LLC; 3LL, H-2^b) heterotopic and orthotopic tumor model systems in C57BL/6 mice replete (CXCR2$^{+/+}$) and deficient in CXCR2 (CXCR2$^{-/-}$). We first demonstrated a correlation of the expression of endogenous ELR$^+$ CXC chemokines with tumor growth and metastatic potential of LLC tumors. Next, we found that LLC primary tumors were significantly reduced in growth in CXCR2$^{-/-}$ mice. Moreover, we found a marked reduction in the spontaneous metastases of heterotopic tumors to the lungs of CXCR2$^{-/-}$ mice. Morphometric analysis of the primary tumors in CXCR2$^{-/-}$ mice demonstrated increased necrosis and reduced vascular density. These findings were further confirmed in CXCR2$^{+/+}$ mice using specific neutralizing Abs to CXCR2. The results of these studies support the notion that CXCR2 mediates the angiogenic activity of ELR$^+$ CXC chemokines in a preclinical model of lung cancer. ***The Journal of Immunology,*** **2004, 172: 2853–2860.**

Although lung cancer, and particularly primary nonsmall cell lung cancer (NSCLC),[3] is the leading cause of malignancy-related mortality in the U.S. (1), the biology of this devastating disease is complex and poorly understood. NSCLC metastases to regional lymph nodes, liver, adrenal glands, contralateral lung, brain, and bone marrow is a key factor in the virulence of this cancer (2, 3). Angiogenesis is felt to play an important role in tumor growth and metastasis. CXCL8 (IL-8) has been determined to be a significant angiogenic factor contributing to overall tumor-derived angiogenic activity in a variety of human tumors (4–10). Furthermore, CXCL1, 2, 3 (growth-related oncogene-α, β, γ) and CXCL5 (epithelial-neutrophil-activating peptide-78), other Glu-Leu-Arg$^+$ (ELR$^+$) CXC chemokines, have also been demonstrated to be equally important in several human tumors and tumor model systems in mice (11–13). These findings demonstrated the importance of different angiogenic ELR$^+$ CXC chemokines in mediating tumor-derived angiogenesis. Thus, tumor cells can use distinct angiogenic ELR$^+$ CXC chemokines to mediate their tumorigenic potential.

We have previously shown that members of the ELR$^+$ CXC chemokine family, including CXCL1, 2, 3; CXCL5; CXCL6 (granulocyte chemotactic protein 2); and CXCL8, can mediate angiogenesis in the absence of preceding inflammation (11, 14). We have also shown that CXCR2 is the receptor responsible for ELR$^+$ CXC chemokine-mediated angiogenesis (15).

We hypothesized that CXCR2 in vivo mediates the proangiogenic effects of ELR$^+$ CXC chemokines during tumorigenesis. We demonstrate that there is a correlation of the expression of endogenous ELR$^+$ CXC chemokines that parallels tumor growth and metastatic potential of Lewis lung cancer (LLC) tumors in CXCR2$^{+/+}$ mice. We also show that LLC primary tumors have significantly reduced growth in CXCR2$^{-/-}$ mice at 4 wk. Moreover, we found a marked reduction in the spontaneous metastases of heterotopic tumors to the lungs of CXCR2$^{-/-}$ mice. Morphometric analysis of the primary tumors in CXCR2$^{-/-}$ mice demonstrated increased areas of necrosis and reduced vascular density, as compared with tumor grown in CXCR2$^{+/+}$ mice. These findings were further confirmed in CXCR2$^{+/+}$ mice in the presence of specific neutralizing Abs to CXCR2. The results of these studies support the notion that CXCR2 mediates the angiogenic activity of ELR$^+$ CXC chemokines in a preclinical model of lung cancer, and highlights the importance of developing strategies to attenuate CXCR2 biology in NSCLC.

Materials and Methods

Abs and Ab generation

Polyclonal goat anti-murine CXCR2 (mCXCR2) was produced by the immunization of a goat with a peptide containing the ligand-binding sequence Met-Gly-Glu-Phe-Lys-Val-Asp-Lys-Phe-Asn-Ile-Glu-Asp-Phe-Phe-Ser-Gly of CXCR2. Direct ELISA was used to evaluate antisera titers, and sera were used for Western blot, ELISA, and neutralization assays when titers had reached greater than 1/1,000,000. The anti-CXCR2 Abs have been used previously to block mCXCR2 in vivo, and have been shown to detect CXCR2 by Western blot and fluorescence-activated cell-sorting analysis of neutrophils in vivo (16–18). The anti-CXCR2 Ab has been shown to be neutralizing using both in vitro neutrophil chemotaxis assay and in vivo by abrogating the influx of neutrophils into the peritoneum of normal mice in response to exogenous ELR$^+$ murine CXC chemokines (16–18). In vivo

*Division of Pulmonary and Critical Care Medicine and †Department of Pathology and Laboratory Medicine, David Geffen School of Medicine, University of California, Los Angeles, CA 90024

Received for publication August 13, 2003. Accepted for publication December 16, 2003.

The costs of publication of this article were defrayed in part by the payment of page charges. This article must therefore be hereby marked *advertisement* in accordance with 18 U.S.C. Section 1734 solely to indicate this fact.

[1] This work was supported, in part, by National Institutes of Health Grants P50HL67665, HL03906 (to M.P.K), HL04493 (to J.A.B.), P50CA90388, P50HL67665, HL66027, and CA87879 (to R.M.S.).

[2] Address correspondence and reprint requests to Dr. Robert M. Strieter, Division of Pulmonary and Critical Care Medicine, David Geffen School of Medicine, University of California, 900 Veteran Avenue, 14-154 Warren Hall, Box 711922, Los Angeles, CA 90024-1922. E-mail address: rstrieter@mednet.ucla.edu

[3] Abbreviations used in this paper: NSCLC, nonsmall cell lung cancer; ELR, Glu-Leu-Arg; LLC, Lewis lung cancer; mCXCR, murine CXCR; VEGF, vascular endothelial growth factor.

0022-1767/04/$02.00

administration of anti-CXCR2 Abs inhibits pulmonary neutrophil sequestration in murine models of Aspergillosis, *Nocardia*, and *Pseudomonas* pneumonia and prevented the influx of neutrophils in urine and the kidney in a murine model of *Escherichia coli* urinary tract infection and into the lung in ventilator-induced lung injury (16–19). Moreover, i.p. administration of this Ab did not alter peripheral blood neutrophil counts (16–18). A total of 1 ml of antiserum against mCXCR2 and control Ab is ~10 mg of IgG.

Anti-factor VIII-related Ag and appropriate control Abs were purchased from DAKO (Carpenteria, CA).

ELISA

The quantity of murine CXCL1, CXCL 2/3, and vascular endothelial growth factor (VEGF) present in tissue homogenates was determined by specific ELISA, using a modification of the double-ligand method, as previously described (19–24). Briefly, flat-bottom 96-well microtiter plates were coated with 50 μl/well of specific polyclonal anti-mouse CXCL1, CXCL2/3, or VEGF (R&D Systems, Minneapolis, MN) (1 μg/ml in 0.6 M of NaCl, 0.26 M of H_3BO_3, and 0.08 N of NaOH, pH 9.6) for 24 h at 4°C, and then washed with PBS, pH 7.5, plus 0.05% Tween 20 (wash buffer). Plates were blocked with 2% BSA in PBS for 1 h at 37°C and then washed three times with wash buffer. A total of 50 μl of sample (1:10 and neat) was added, and the plates were incubated at 37°C for 1 h. Plates were washed three times; 50 μl of biotinylated polyclonal anti-human or mouse CXCL1, CXCL2/3, or VEGF (R&D Systems) (3.5 ng/μl in PBS, pH 7.5, 0.05% Tween 20, and 2% FBS) was added; and plates were incubated at 37°C for 45 min. Plates were washed three times; streptavidin-peroxidase conjugate was added; and the plates were incubated for 30 min at 37°C. Plates were washed again, and 100 μl of 3, 3′, 5, 5′-tetramethylbenzidine chromogenic substrate was added. Plates were incubated at room temperature to the desired extinction, and the reactions were terminated by the addition of 100 μl/well of 1 M of H_3PO_4. Plates were read at 450 nm in an automated microtiter plate reader, and the amount of mouse CXCL1, CXCL2/3, or VEGF present was determined by interpolation of a standard curve generated by known amounts of recombinant mouse CXCL1, CXCL2/3, or VEGF (R&D Systems), respectively. The sensitivity for the mouse CXCL1/2, CXCL1, or VEGF ELISAs was >50 pg/ml, and this assay failed to cross-react with a panel of other known cytokines and chemokines.

Heterotopic and orthotopic LLC model

C57BL/6 CXCR2$^{-/-}$ and CXCR2$^{+/+}$ mice (6–8 wk old, derived from the strain developed at Genentech (South San Francisco, CA) by Cacalano et al. (25), a gift from R. Terkeltaub (University of California, San Diego, CA) and maintained by A. Richmond (Vanderbilt University, Nashville, TN)) were injected either s.c. (heterotopic; 10^6 cells per 100 μl) into one flank or transthoracically (orthotopic; 10^4 cells per 25 μl) into the left lung with LLC cells using a modification, as previously described (11, 20, 26, 27). The animals were maintained in sterile laminar flow rooms and sacrificed in groups of 10. Animals were evaluated for evidence of NSCLC metastases. In subsequent experiments, LLC tumor-bearing C57BL/6 mice were exposed to i.p. injections of 500 μl of either neutralizing goat anti-mCXCR2, control (preimmune) serum, or no treatment, every day, for 28 days, starting at the time of xenoengraftment. Subcutaneous heterotopically placed tumors were dissected from the mice and measured with a Thorpe caliper (Biomedical Research Instruments, Rockville, MD). Tumor volume was calculated using the formula: volume = $(d_1 \times d_2 \times d_3) \times 0.5236$, where d_n represents the three orthogonal diameter measurements. Orthotopically placed lung tumors were histologically evaluated. Tumor and tissue specimens were processed in the following manner: 1) fixed in 4% paraformaldehyde for histologic analysis and immunohistochemistry; 2) the tumor was processed to a single cell suspension for subsequent FACS analysis of factor VIII-related Ag; 3) processed for protein analysis by ELISA for cytokine levels, as previously described (19–24).

FACS analysis of tumors

Analysis of tumor-derived factor VIII-related Ag, single cell suspension preparations was made using a method, as previously described (19, 24). Briefly, heterotopic tumors or lungs containing orthotopic tumors were harvested at 8 wk from animals who had been treated with either control/preimmune or anti-mCXCR2 Abs. Tissue was minced with scissors to a fine slurry in 15 ml of digestion buffer (RPMI 1640, 5% FCS, 1 mg/ml collagenase (Boehringer Mannheim, Indianapolis, IN), and 30 μg/ml DNase (Sigma-Aldrich, St. Louis, MO)). Tissue slurry was enzymatically digested for 45 min at 37°C. Any undigested fragments were further dispersed by drawing the solution up and down through the bore of a 10-ml syringe. The total cell suspension was pelleted and resuspended in FACS analysis buffer. Cell counts and viability were determined using trypan blue exclusion on a hemocytometer. Single cell suspensions were stained with primary rabbit anti-factor VIII-related Ag Abs (Sigma-Aldrich), goat anti-mCXCR2, and isotype controls. The secondary Abs used for these experiments were Alexa 488 (FITC anti-rabbit) (Molecular Probes, Eugene, OR) and PE swine anti-goat (Caltag Laboratories, South San Francisco, CA). Samples were also stained with tricolor conjugated anti-murine CD45 (Caltag Laboratories), with PE-conjugated CD3, CD4, CD8A, NK1.1, Ly-6 (BD Biosciences, San Jose, CA), or MAC519 (Serotec, Raleigh, NC). Cells were analyzed on a FACScan flow cytometer (BD Biosciences) using CellQuest software (BD Biosciences), as previously described (19, 24).

Proliferation of LLC cells

Proliferation of LLC cells was assessed using 96-well culture plates seeded with either 1000 or 5000 LLC cells/well, which were starved overnight in growth medium containing 1% FCS. The next morning, medium containing 1 or 10% serum was added to the cultures together with varying concentrations of CXCL1, CXCL2/3, or anti-CXCR2 (0.001–100 ng/ml), and the cells were allowed to grow for 72 h. At this time, 1 μCi/well [^{3}H]thymidine was added, and the cultures were incubated for a further 18 h. Finally, the cells were harvested using a cell harvester, and [^{3}H]thymidine incorporation was quantitated by scintillation counting.

Immunolocalization of factor VIII-related Ag

Paraffin-embedded tissue from control and bleomycin-treated lung was processed for immunohistochemical localization of factor VIII-related Ag, as previously described (14). Briefly, tissue sections were dewaxed with xylene and rehydrated through graded concentrations of ethanol. Slides were blocked with normal goat serum (BioGenex, San Ramon, CA), and overlaid with 1/500 dilution of either control (rabbit) or polyclonal rabbit anti-factor VIII-related Ag Abs. Slides were then rinsed and overlaid with secondary biotinylated goat anti-rabbit IgG (1/35) and incubated for 60 min. After washing with TBS, slides were overlaid with a 1/35 dilution of alkaline phosphatase conjugated to streptavidin (BioGenex Laboratories, San Ramon, CA) and incubated for 60 min. Fast Red (BioGenex Laboratories) reagent was used for chromogenic localization of factor VIII-related Ag. After optimal color development, sections were immersed in sterile water, counterstained with Lerners hematoxylin, and coverslipped using an aqueous mounting solution.

Quantitation of vessel density

Quantitation of vessel density was performed using a modification of the previously described method (11). Briefly, slides were stained for factor VIII-related Ag, as outlined above. Tumor specimens were scanned at low magnification (×40) to identify vascular hot spots. Areas of greatest vessel density were then examined under higher magnification (×200) and counted. Any distinct areas of positive staining for factor VIII-related Ag were counted as a single vessel. Results were expressed as the number of vessels per high-powered field (×200).

Immunohistochemistry for CXCR2

Human NSCLC and murine LLC tumor specimens were fixed in 4% paraformaldehyde for 24 h. Paraffin-embedded tissue sections were dewaxed with xylene and rehydrated through graded concentrations of ethanol. Twenty specimens of human stage I and II squamous cell carcinoma and 20 samples of human stage I and II adenocarcinomas were then stained for CXCR2 using the Vectastain ABC system (Vector Laboratories, Burlingame, CA). Briefly, nonspecific binding sites were blocked with powerblock (BioGenex Laboratories), washed, and overlaid with 1/100 dilution of either control (rabbit) or rabbit anti-human CXCR2. Slides were then rinsed and overlaid with secondary biotinylated goat anti-rabbit IgG and incubated for 30 min. After washing twice with PBS, slides were overlaid with Vectastain ABC systems peroxidase-conjugated streptavidin and incubated for 30 min. The 3,3′-diaminobenzidine tetrahydrochloride reagent was used for chromogenic localization of CXCR2. After optimal color development, sections were immersed in sterile water, counterstained with Mayer's hematoxylin, and coverslipped with mounting solution.

Morphometric analysis of metastases and tumor necrosis

For analysis of lung metastases and necrotic areas, morphometric analysis was performed on at least 16 separate H&E-stained sections taken 60 μm apart from each of five different animals under ×200 magnification. An Olympus BH-2 microscope coupled to a Sony 3CCD camera was used to capture images that were then analyzed for total area of metastatic lesions using the NIH Image 1.55 software. For determination of tumor necrosis, the average percentage of necrotic area per high power field (×200) for each tumor was determined by morphometric analysis, and this number

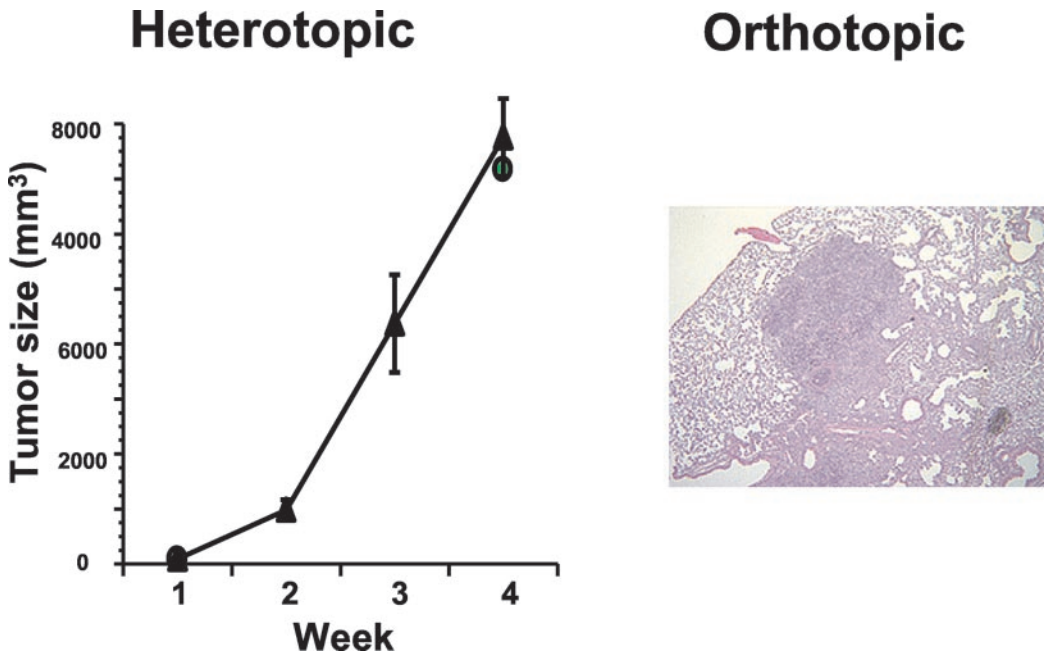

FIGURE 1. Tumor growth over 4 wk in the heterotopic and orthotopic LLC models. Heterotopic tumor growth was measured weekly; orthotopic growth was assessed histologically at the end of 4 wk. Heterotopic tumor volume was calculated using the formula: volume = $(d_1 \times d_2 \times d_3) \times 0.5236$), where d_n represents the three orthogonal diameter measurements.

was then multiplied by the tumor area yielding the average necrotic area for each tumor.

Statistical analysis

The animal studies involved 10 mice for each treatment group. Data were analyzed on a Dell PC computer using the Statview 5.0 statistical package (Abacus Concepts, Berkeley, CA). Comparisons were evaluated by the unpaired *t* test. All group comparisons were evaluated by nonparametric analysis using either the Mann-Whitney analyses or the Kruskal-Wallis test with the post hoc analysis, Dunn for statistical significance. Data were considered statistically significant if *p* values were 0.05 or less, designated by an asterisk (*).

Results

Both the heterotopic and orthotopic LLC tumors demonstrate significant growth over 4-wk period of time

In the heterotopic model, tumor size was determined by direct measurement and tumors showed significant growth over a 4-wk period (Fig. 1). In the orthotopic model, tumor size was assessed histologically and also demonstrated marked growth over a 4-wk period with the tumor occupying a significant portion of the left lung (Fig. 1)

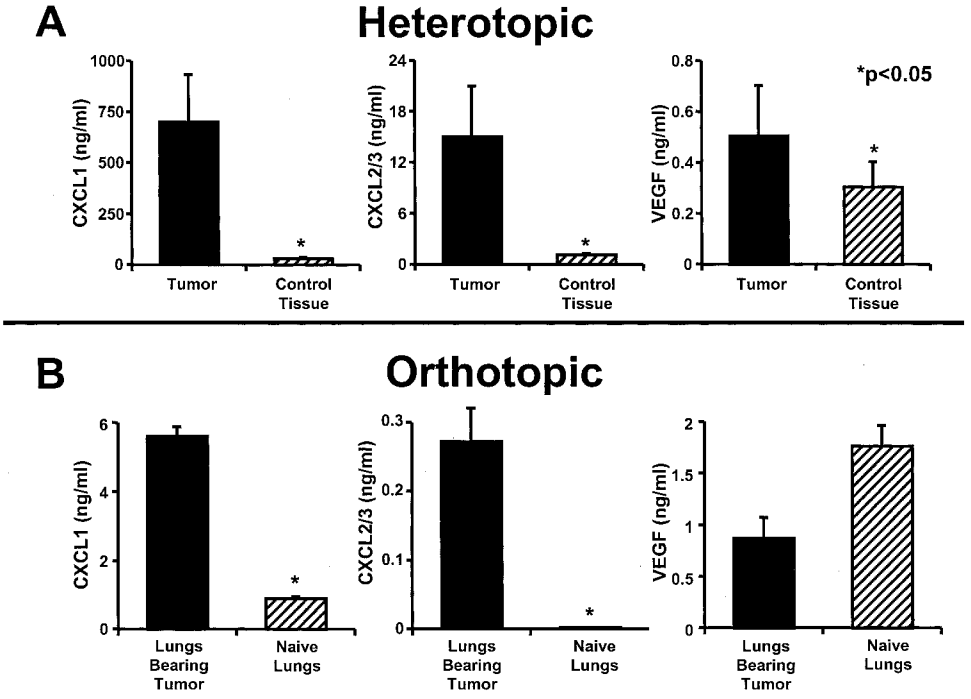

FIGURE 2. Levels of CXCL1 and CXCL2/3 are elevated in the heterotopic and orthotopic LLC models. Protein levels were measured by ELISA from heterotopic LLC tumors or from the lung bearing the tumor in the orthotopic model.

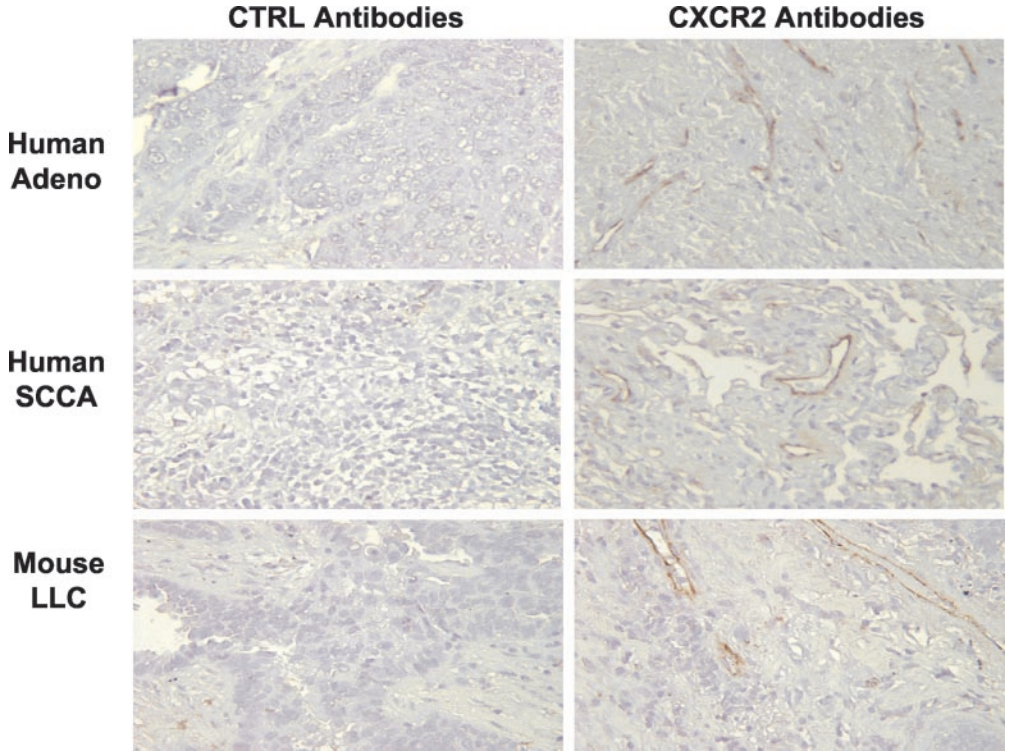

FIGURE 3. Photomicrograph of the immunolocalization of CXCR2 in human adenocarcinoma, NSCLC, and mouse LLC tumors demonstrating immunolocalization to vascular endothelium (×40).

CXCL1 and CXCL2/3 are elevated in the heterotopic and orthotopic LLC tumors

We next measured levels of CXCL1 and CXCL2/3 from orthotopic and heterotopic tumors by specific ELISA standardized to volume of biopsy. For the heterotopic model, a punch biopsy of adjacent skin of similar size to the tumor was used for evaluation. For the orthotopic model, the tumor-bearing lung was compared with a naive lung without tumor. Both CXCL1 and CXCL2/3 were significantly elevated at 4 wk as compared with control tissue (Fig. 2) in both the heterotopic and orthotopic tumors. We also measured VEGF levels from both orthotopic and heterotopic tumors and found that VEGF levels were elevated in the heterotopic tumors, but not the orthotopic tumors, as compared with control tissue.

CXCR2 is predominantly expressed on endothelium within tumors

Because both CXCL1 and CXCL2/3 were significantly elevated at 4 wk as compared with control tissue, we next assessed the predominant cells expressing CXCR2, the common receptor for both of these ligands. We found that the predominant cells expressing CXCR2 were vascular endothelial cells within the tumors, suggesting that CXCR2 has a role in angiogenesis associated with tumor growth (Fig. 3). This was confirmed by FACS analysis of single cell suspensions of heterotopic tumors, demonstrating that CXCR2 is expressed on the majority of cells that express factor VIII-related Ag (Table I).

LLC tumor growth is attenuated in CXCR2$^{-/-}$ mice

To further evaluate the role of CXCR2 expression on tumor growth, we measured both orthotopic and heterotopic tumor growth in CXCR2$^{-/-}$ mice as compared with tumor growth in wild-type control mice. There was a significant reduction in tumor growth in CXCR2$^{-/-}$ mice as compared with wild-type control animals (Fig. 4). To confirm these findings, we passively immunized mice with orthotopic tumors and found that neutralization of CXCR2 using neutralizing Abs led to a significant reduction in tumor growth as compared with control-treated animals (Fig. 4*B*), confirming the findings in the CXCR2$^{-/-}$ mice. Similarly, neutralization of CXCR2 leads to a reduction in heterotopic tumor growth.

Depletion of CXCR2 is associated with increased tumor necrosis

To further examine the mechanism of inhibition of tumor growth, we next assessed tumor necrosis in the context of the presence or absence of CXCR2 in the heterotopic model. We found that there was an increase in tumor necrosis in CXCR2$^{-/-}$ mice as compared with wild-type controls (Figs. 5). To confirm these findings in a more biologically relevant system, we next performed in vivo neutralization studies using polyclonal Abs directed against CXCR2 in heterotopic tumor model. Similar to the CXCR2$^{-/-}$ mice, neutralization of CXCR2 by passive immunization led to an increase in tumor necrosis (Fig. 5).

CXCL1 and CXCL2/3 have no effect on LLC cell proliferation

Having shown that neutralization of CXCR2 inhibited tumor growth, we were next interested to know whether the ligands CXCL1 and CXCL2/3 have an effect on tumor cell proliferation. LLC cells were stimulated with various concentrations of CXCL1 and CXCL2/3. Proliferation was measured using incorporation of [^{3}H]thymidine. CXCL1 and CXCL2/3 had no effect on LLC proliferation (data not shown). Furthermore,

Table I. *FACS analysis of single cell isolates from heterotopic LLC tumors double stained for factor VIII-related Ag and CXCR2 and gated on the factor VIII-related Ag-positive cells*

	CXCR2 % Positive	CXCR2 % Negative
Factor VIII positive	98.94 ± 0.09	1.06 ± 0.01

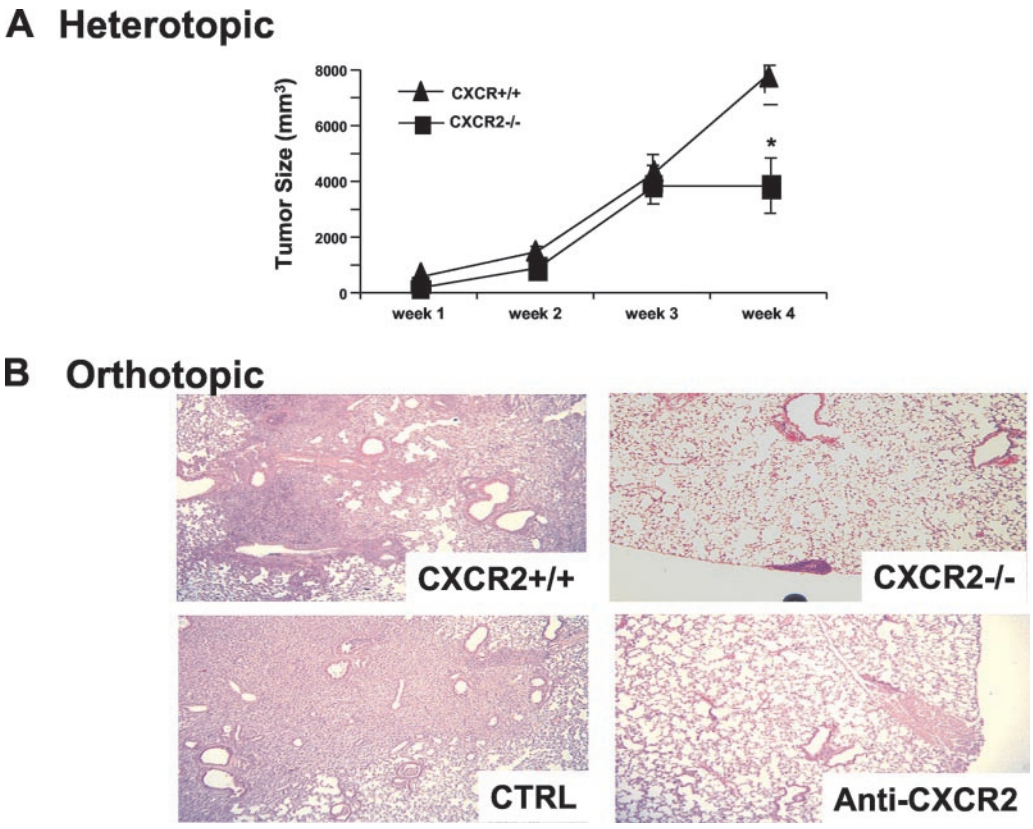

FIGURE 4. *A,* Inhibition of heterotopic LLC tumor growth over 4 wk in CXCR2$^{-/-}$ mice. *B,* Inhibition of orthotopic LLC tumor growth at 4 wk in CXCR2$^{-/-}$ mice and in mice treated with neutralizing anti-CXCR2 Abs. Ab-treated mice were passively immunized with either goat anti-mCXCR2 or normal goat serum every day for 4 wk.

anti-CXCR2 had no effect on tumor proliferation (data not shown).

Depletion of CXCR2 inhibits angiogenesis in LLC tumors and has no effect on intratumor leukocyte infiltration

To further assess the mechanism for the reduced tumor growth of LLC in CXCR2$^{-/-}$ mice and following inhibition of CXCR2 with specific Abs, we next looked at the role of CXCR2 depletion on tumor angiogenesis and leukocyte infiltration. There was a significant decrease in angiogenesis, as determined by vessel counting and FACS analysis of factor VIII-related Ag in tumor homogenates of CXCR2-depleted as compared with control tumors (Fig. 6). CXCL1 and CXCL2/3 are potent neutrophil chemoattractants. To exclude the possibility that the beneficial effect of CXCR2 depletion was due to an alteration in neutrophil recruitment, we performed leukocyte subpopulation analysis in tumors from CXCR2$^{-/-}$ mice or mice treated with anti-mCXCR2 as compared with CXCR2$^{+/+}$ control mice. Analysis of leukocyte subpopulations demonstrated no significant difference in the populations of leukocytes present in tumors under these circumstances (Table II).

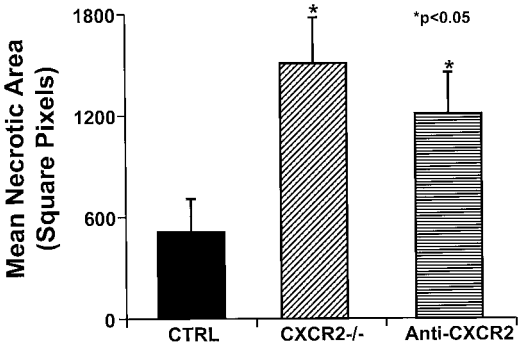

FIGURE 5. Mean necrotic area in heterotopic LLC tumors in CXCR2$^{-/-}$ or in mice treated with neutralizing anti-CXCR2 Abs as compared with control-treated mice. Ab-treated mice were passively immunized with either goat anti-mCXCR2 or normal goat serum every day for 4 wk. Mean necrotic area was assessed by morphometric analysis and expressed as square pixels.

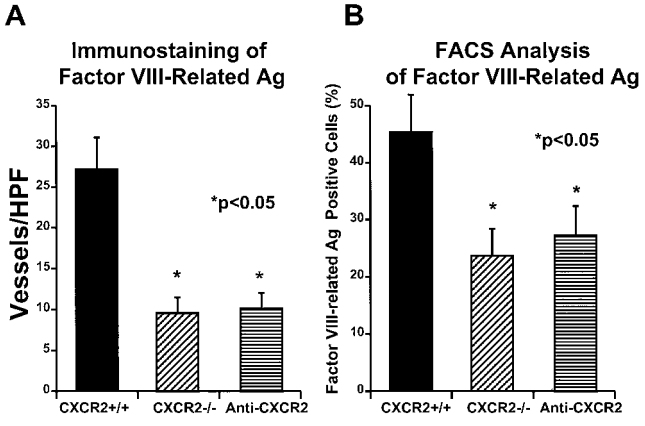

FIGURE 6. Reduction in factor VIII-related Ag-expressing cells in heterotopic tumors from CXCR2$^{-/-}$ mice or mice passively immunized with anti-CXCR2 Abs as compared with controls at 4 wk. Ab-treated mice were passively immunized with either goat anti-mCXCR2 or normal goat serum every day for 4 wk. *A,* Vessel density, as assessed by hot spot counting, in sections of heterotopic LLC tumors. $n = 10$ sections per group. *B,* FACS analysis of factor VIII-related Ag expression in single cell suspensions of heterotopic LLC tumors. $n = 6$ in each group.

Table II. *FACS analysis of single cell isolates from LLC tumors in either control or CXCR2$^{-/-}$ mice*[a]

Tumor	CD45$^+$	CD3$^+$	CD4$^+$	CD8$^+$	NK$^+$	PMN$^+$	MØ$^+$
Control mice	10.4 ± 1.0	4.1 ± 0.63	2.3 ± 0.15	1.8 ± .11	0.03 ± 0.01	2.7 ± 0.33	3.7 ± 1.7
CXCR2$^{-/-}$ mice	9.8 ± 0.98	4.0 ± 0.55	2.5 ± 0.09	1.5 ± 0.21	0.049 ± 0.009	2.4 ± 0.27	3.7 ± 0.17

[a] Numbers represent percentage of positive staining.

Depletion of CXCR2 is associated with decreased lung metastases in the heterotopic LLC model

We were next interested in the wider implications of inhibition of growth of the primary tumor. We therefore looked at the effects of CXCR2 depletion on metastases using the heterotopic model. We counted lung metastases in CXCR2$^{-/-}$ mice or in mice that had been treated with anti-CXCR2 Abs. There was a significant reduction in the numbers of lung metastases as compared with control mice (Fig. 7). This supports the notion that CXCR2-mediated angiogenesis is important for both primary tumor growth and metastasis.

Discussion

The CXC chemokines can be divided into two groups on the basis of a structure/function domain consisting of the presence or absence of 3 aa residues (Glu-Leu-Arg; ELR motif) that precedes the first cysteine amino acid residue in the primary structure of these cytokines (28–34). The ELR$^+$ CXC chemokines are chemoattractants for neutrophils and act as potent angiogenic factors (35–37). In contrast, the IFN-inducible ELR$^-$ CXC chemokines are chemoattractants for mononuclear cells and are potent inhibitors of angiogenesis (37, 38).

CXCR2 has been shown to bind all of the ELR$^+$ CXC chemokines (39–41). We have previously demonstrated the importance of CXCR2 in mediating ELR$^+$ CXC chemokine-induced angiogenesis in vivo, by the lack of angiogenic activity induced by ELR$^+$ CXC chemokines in the presence of neutralizing Abs to CXCR2 in the rat corneal micropocket assay, or in the corneas of CXCR2$^{-/-}$ mice (42). Li et al. (43) have shown that CXCL8 induces endothelial cell tube formation and inhibits apoptosis in endothelial cells via CXCR1 and CXCR2. Furthermore, significant delays in wound healing, including epithelialization and decreased neovascularization, have been described in CXCR2$^{-/-}$ mice (44).

Angiogenesis is necessary for growth of all solid tumors, and the net vascularization of a tumor is dependent upon the balance of the expression of angiogenic and angiostatic factors. We have shown that the CXC chemokines, CXCL5 and CXCL8, are important factors in angiogenesis and tumor growth (11, 14). Therefore, it is a logical extension of these observations that inhibition of the common receptor for the angiogenic CXC chemokines would have a similar effect. The attractive feature of targeting the receptor is the fact that it leads to inhibition of several ELR$^+$ chemokine ligands at once. Saijo et al. (45) have shown that transfection of LLC cells with IL-1β leads to hyperneovascularization as compared with wild-type LLC tumors and that heterotopic growth of these tumors could be attenuated using Abs to CXCR2. These authors did not, however, directly look at the effect of this treatment on tumor necrosis, angiogenesis, or metastases. Although it is possible that CXC chemokines inhibit apoptosis of LLC cells via CXCR2, our results in the CXCR2$^{-/-}$ mice suggest that this is not a significant factor. In the CXCR2$^{-/-}$ mice, CXCR2 is still expressed on the LLC cells, and therefore CXC chemokines could still exert an antiapoptotic effect. The fact that the tumor growth was inhibited in the CXCR2$^{-/-}$ mice suggests that it is CXCR2 on host cells (i.e., endothelial cells) that is the primary determinant of the effect of CXC chemokines on tumor growth.

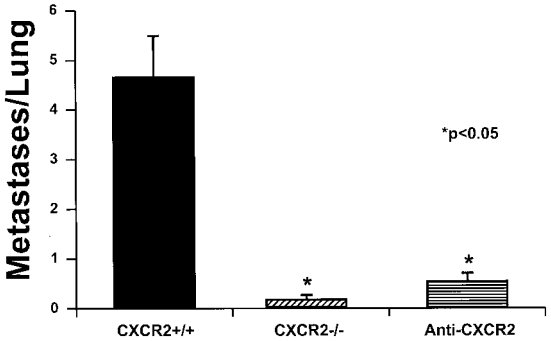

FIGURE 7. Reduction in the number of lung metastases in heterotopic LLC tumor-bearing mice in either CXCR2$^{-/-}$ mice or mice passively immunized with anti-CXCR2 Abs as compared with controls at 4 wk. Ab-treated mice were passively immunized with either goat anti-mCXCR2 or normal goat serum every day for 4 wk. Metastases were counted at magnification of ×40 on histologic sections of lungs from tumor-bearing mice. $n = 2$ sections per mouse and 6 mice per group.

The heterotopic lung cancer model has been criticized as not being truly representative of lung cancer, as the primary tumor is anatomically distant from the lung. To overcome this concern, we also used an orthotopic model in which the primary tumor is implanted directly in the lung. We found similar patterns of tumor growth with these two models. Furthermore, the two models had similar changes in tumor growth, vessel density, and tumor necrosis when CXCR2 biology was attenuated. Using the heterotopic model, we also demonstrated a decrease in metastases to the lung, indicating the importance of angiogenesis to the development of metastases. Furthermore, recent evidence suggests that the size of a stage I NSCLC does not correlate with prognosis, and would suggest that the vessel density may be a more important determinant of metastatic potential (46). However, we cannot exclude the possibility that the decrease in metastases is due to either a decrease in the size of the primary tumor or a decrease in the growth of metastatic cells once they reach the lung.

The ELR$^+$ CXC chemokines are potent neutrophil chemoattractants in addition to their angiogenic effects. Inhibition of CXCR2 did not lead to any significant changes in intratumor leukocytes. This is similar to what we have previously shown in a murine model of pulmonary fibrosis in which inhibition of CXCL2/3 reduced fibrosis via inhibition of angiogenesis without any alteration in pulmonary neutrophils (23). One might speculate that inhibition of CXCR2 could lead to defects in host defense, as has been shown in animal models of pneumonia, and that such a strategy could be detrimental in a potentially immunocompromised patient (16–18). In the human setting, however, this concern is obviated by the presence of CXCR1 on neutrophils, which would allow CXCL8 and CXCL6 to function normally as neutrophil chemoattractants in the setting of infection.

Although clinical trials of inhibition of angiogenesis have been disappointing to date, most of the strategies used have targeted a single mediator, specifically VEGF (47, 48). These studies have

demonstrated the limitations of targeting a single mediator (47, 48). Similarly, the appropriate biological end point for effective antiangiogenic therapy is not clear (47). Although our results show a significant reduction in tumor size with inhibition of CXCR2, we also found that there was a significant increase in tumor necrosis with inhibition of CXCR2. This suggests that the traditional end points of tumor size should not be the only end point used in determining the efficacy of antiangiogenic therapy.

Our results demonstrate that targeting several angiogenic mediators at once is an attractive therapeutic option. Our Ab studies demonstrate that total ablation of CXCR2 before tumor development, as seen in the $CXCR2^{-/-}$ mice, is not necessary and that the results in the knockout mice can be replicated using an Ab approach even after tumor implantation. Recent reports of acquired resistance to antiangiogenic therapy underscore the need for development of strategies that have the ability to target multiple pathways and/or mediators in angiogenesis (49, 50). Our findings demonstrate that targeting CXCR2 may represent a potential target in the development of novel antiangiogenesis agents.

References

1. Devesa, S. S., W. J. Blot, B. J. Stone, B. A. Miller, R. E. Tarone, and J. F. Fraumeni, Jr. 1995. Recent cancer trends in the United States. *J. Natl. Cancer Inst. 87:175*.
2. Fidler, I. J. 1990. Critical factors in the biology of human cancer metastasis: Twenty-Eighth G. H. A. Clowes Memorial Award Lecture. *Cancer Res. 50:6130*.
3. Fidler, I. J. 1999. Critical determinants of cancer metastasis: rationale for therapy. *Cancer Chemother. Pharmacol. 43:S3*.
4. Smith, D. R., P. J. Polverini, S. L. Kunkel, M. B. Orringer, R. I. Whyte, M. D. Burdick, C. A. Wilke, and R. M. Strieter. 1994. Inhibition of interleukin 8 attenuates angiogenesis in bronchogenic carcinoma. *J. Exp. Med. 179:1409*.
5. Antony, V. B., J. W. Hott, S. W. Godbey, and K. Holm. 1996. Angiogenesis in mesotheliomas: role of mesothelial cell derived IL-8. *Chest 109:21S*.
6. Ferrer, F. A., L. J. Miller, R. I. Andrawis, S. H. Kurtzman, P. C. Albertsen, V. P. Laudone, and D. L. Kreutzer. 1998. Angiogenesis and prostate cancer: in vivo and in vitro expression of angiogenesis factors by prostate cancer cells. *Urology 51:161*.
7. Yatsunami, J., N. Tsuruta, K. Ogata, K. Wakamatsu, K. Takayama, M. Kawasaki, Y. Nakanishi, N. Hara, and S. Hayashi. 1997. Interleukin-8 participates in angiogenesis in non-small cell, but not small cell carcinoma of the lung. *Cancer Lett. 120:101*.
8. Yoneda, J., H. Kuniyasu, M. A. Crispens, J. E. Price, C. D. Bucana, and I. J. Fidler. 1998. Expression of angiogenesis-related genes and progression of human ovarian carcinomas in nude mice. *J. Natl. Cancer Inst. 90:447*.
9. Fox, S. H., G. F. Whalen, M. M. Sanders, J. A. Burleson, K. Jennings, S. Kurtzman, and D. Kreutzer. 1998. Angiogenesis in normal tissue adjacent to colon cancer. *J. Surg. Oncol. 69:230*.
10. Bar-Eli, M. 1999. Role of interleukin-8 in tumor growth and metastasis of human melanoma. *Pathobiology 67:12*.
11. Arenberg, D. A., M. P. Keane, B. DiGiovine, S. L. Kunkel, S. B. Morris, Y. Y. Xue, M. D. Burdick, M. C. Glass, M. D. Iannettoni, and R. M. Strieter. 1998. Epithelial-Neutrophil activating peptide (ENA-78) is an important angiogenic factor in non-small cell lung cancer. *J. Clin. Invest. 102:465*.
12. Moore, B. B., D. A. Arenberg, K. Stoy, T. Morgan, C. L. Addison, S. B. Morris, M. Glass, C. Wilke, Y. Y. Xue, S. Sitterding, et al. 1999. Distinct CXC chemokines mediate tumorigenicity of prostate cancer cells. *Am. J. Pathol. 154:1503*.
13. Luan, J., R. Shattuck-Brandt, H. Haghnegahdar, J. D. Owen, R. Strieter, M. Burdick, C. Nirodi, D. Beauchamp, K. N. Johnson, and A. Richmond. 1997. Mechanism and biological significance of constitutive expression of MGSA/GRO chemokines in malignant melanoma tumor progression. *J. Leukocyte Biol. 62:588*.
14. Arenberg, D. A., S. L. Kunkel, P. J. Polverini, M. Glass, M. D. Burdick, and R. M. Strieter. 1996. Inhibition of interleukin-8 reduces tumorigenesis of human non-small cell lung cancer in SCID mice. *J. Clin. Invest. 97:2792*.
15. Addison, C. L., T. O. Daniel, M. D. Burdick, H. Liu, J. E. Ehlert, Y. Y. Xue, L. Buechi, A. Walz, A. Richmond, and R. M. Strieter. 2000. The CXC chemokine receptor 2, CXCR2, is the putative receptor for ELR^+ CXC chemokine-induced angiogenic activity. *J. Immunol. 165:5269*.
16. Mehrad, B., R. M. Strieter, T. A. Moore, W. C. Tsai, S. A. Lira, and T. J. Standiford. 1999. CXC chemokine receptor-2 ligands are necessary components of neutrophil-mediated host defense in invasive pulmonary aspergillosis. *J. Immunol. 163:6086*.
17. Moore, T. A., M. W. Newstead, R. M. Strieter, B. Mehrad, B. L. Beaman, and T. J. Standiford. 2000. Bacterial clearance and survival are dependent on CXC chemokine receptor-2 ligands in a murine model of pulmonary *Nocardia asteroides* infection. *J. Immunol. 164:908*.
18. Tsai, W. C., R. M. Strieter, B. Mehrad, M. W. Newstead, X. Zeng, and T. J. Standiford. 2000. CXC chemokine receptor CXCR2 is essential for protective innate host response in murine *Pseudomonas aeruginosa* pneumonia. *Infect. Immun. 68:4289*.
19. Belperio, J. A., M. P. Keane, M. D. Burdick, V. Londhe, Y. Y. Xue, K. Li, R. J. Phillips, and R. M. Strieter. 2002. Critical role for CXCR2 and CXCR2 ligands during the pathogenesis of ventilator-induced lung injury. *J. Clin. Invest. 110:1703*.
20. Phillips, R. J., M. D. Burdick, M. Lutz, J. A. Belperio, M. P. Keane, and R. M. Strieter. 2003. The stromal derived factor-1/CXCL12-CXC chemokine receptor 4 biological axis in non-small cell lung cancer metastases. *Am. J. Respir. Crit. Care Med. 167:1676*.
21. Belperio, J. A., M. Dy, M. D. Burdick, Y. Y. Xue, K. Li, J. A. Elias, and M. P. Keane. 2002. Interaction of IL-13 and C10 in the pathogenesis of bleomycin-induced pulmonary fibrosis. *Am. J. Respir. Cell Mol. Biol. 27:419*.
22. Keane, M. P., D. A. Arenberg, J. P. Lynch, R. I. Whyte, M. D. Iannettoni, M. D. Burdick, C. A. Wilke, S. B. Morris, M. C. Glass, B. DiGiovine, et al. 1997. The CXC chemokines, IL-8 and IP-10, regulate angiogenic activity in idiopathic pulmonary fibrosis. *J. Immunol. 159:1437*.
23. Keane, M. P., J. A. Belperio, T. A. Moore, B. B. Moore, D. A. Arenberg, R. E. Smith, M. D. Burdick, S. L. Kunkel, and R. M. Strieter. 1999. Neutralization of the CXC chemokine, macrophage inflammatory protein-2, attenuates bleomycin-induced pulmonary fibrosis. *J. Immunol. 162:5511*.
24. Keane, M. P., J. A. Belperio, D. A. Arenberg, M. D. Burdick, Z. J. Xu, Y. Y. Xue, and R. M. Strieter. 1999. IFN-γ-inducible protein-10 attenuates bleomycin-induced pulmonary fibrosis via inhibition of angiogenesis. *J. Immunol. 163:5686*.
25. Cacalano, G., J. Lee, K. Kikly, A. M. Ryan, S. Pitts-Meek, B. Hultgren, W. I. Wood, and M. W. Moore. 1994. Neutrophil and B cell expansion in mice that lack the murine IL-8 receptor homolog. *Science 265:682*.
26. Addison, C. L., D. A. Arenberg, S. B. Morris, Y. Y. Xue, M. D. Burdick, M. S. Mulligan, M. D. Iannettoni, and R. M. Strieter. 2000. The CXC chemokine, monokine induced by interferon-γ, inhibits non-small cell lung carcinoma tumor growth and metastasis. *Hum. Gene Ther. 11:247*.
27. Arenberg, D. A., S. L. Kunkel, P. J. Polverini, S. B. Morris, M. D. Burdick, M. C. Glass, D. T. Taub, M. D. Iannettoni, R. I. Whyte, and R. M. Strieter. 1996. Interferon-γ-inducible protein 10 (IP-10) is an angiostatic factor that inhibits human non-small cell lung cancer (NSCLC) tumorigenesis and spontaneous metastases. *J. Exp. Med. 184:981*.
28. Farber, J. M. 1993. HuMIG: a new member of the chemokine family of cytokines. *Biochem. Biophys. Res. Commun. 192:223*.
29. Taub, D. D., and J. J. Oppenheim. 1994. Chemokines, inflammation and immune system. *Ther. Immunol. 1:229*.
30. Proost, P., C. D. Wolf-Peeters, R. Conings, G. Opdenakker, A. Billiau, and J. V. Damme. 1993. Identification of a novel granulocyte chemotactic protein (GCP-1) from human tumor cells: in vitro and in vivo comparison with natural forms of GROa, IP-10, and IL-8. *J. Immunol. 150:1000*.
31. Walz, A., R. Burgener, B. Car, M. Baggiolini, S. L. Kunkel, and R. M. Strieter. 1991. Structure and neutrophil-activating properties of a novel inflammatory peptide (ENA-78) with homology to interleukin-8. *J. Exp. Med. 174:1355*.
32. Strieter, R. M., N. W. Lukacs, T. J. Standiford, and S. L. Kunkel. 1993. Cytokines and lung inflammation. *Thorax 48:765*.
33. Koch, A. E., and R. M. Strieter. 1996. *Chemokines in disease*. R. G. Landes, Biomedical Publishers, Austin, TX.
34. Strieter, R. M., and S. L. Kunkel. 1997. Chemokines in the lung. In *Lung: Scientific Foundations*, 2nd Ed. R. Crystal, J. West, E. Weibel, and P. Barnes, eds. Raven Press, New York, p. 155.
35. Clark-Lewis, I., B. Dewald, T. Geiser, B. Moser, and M. Baggiolini. 1993. Platelet factor 4 binds to interleukin 8 receptors and activates neutrophils when its N terminus is modified with Glu-Leu-Arg. *Proc. Natl. Acad. Sci. USA 90:3574*.
36. Hebert, C. A., R. V. Vitangcol, and J. B. Baker. 1991. Scanning mutagenesis of interleukin-8 identifies a cluster of residues required for receptor binding. *J. Biol. Chem. 266:18989*.
37. Strieter, R. M., P. J. Polverini, S. L. Kunkel, D. A. Arenberg, M. D. Burdick, J. Kasper, J. Dzuiba, J. V. Damme, A. Walz, D. Marriott, et al. 1995. The functional role of the 'ELR' motif in CXC chemokine-mediated angiogenesis. *J. Biol. Chem. 270:27348*.
38. Luster, A. D., S. M. Greenberg, and P. Leder. 1995. The IP-10 chemokine binds to a specific cell surface heparan sulfate shared with platelet factor 4 and inhibits endothelial cell proliferation. *J. Exp. Med. 182:219*.
39. Murphy, P. M., and H. L. Tiffany. 1991. Cloning of complementary DNA encoding a functional human interleukin-8 receptor. *Science 253:1280*.
40. Lee, J., R. Horuk, G. C. Rice, G. L. Bennett, T. Camerato, and W. I. Wood. 1992. Characterization of two high affinity human interleukin-8 receptors. *J. Biol. Chem. 267:16283*.
41. Ahuja, S. K., J. C. Lee, and P. M. Murphy. 1996. CXC chemokines bind to unique sets of selectivity determinants that can function independently and are broadly distributed on multiple domains of human interleukin-8 receptor B: determinants of high affinity binding and receptor activation are distinct. *J. Biol. Chem. 271:225*.

42. Addison, C. L., T. O. Daniel, M. D. Burdick, H. Liu, J. E. Ehlert, Y. Y. Xue, L. Buechi, A. Walz, A. Richmond, and R. M. Strieter. 2000. The CXC chemokine receptor 2, CXCR2, is the putative receptor for ELR$^+$ CXC chemokine-induced angiogenic activity. *J. Immunol. 165:5269.*

43. Li, A., S. Dubey, M. L. Varney, B. J. Dave, and R. K. Singh. 2003. IL-8 directly enhanced endothelial cell survival, proliferation, and matrix metalloproteinases production and regulated angiogenesis. *J. Immunol. 170:3369.*

44. Devalaraja, R. M., L. B. Nanney, J. Du, Q. Qian, Y. Yu, M. N. Devalaraja, and A. Richmond. 2000. Delayed wound healing in CXCR2 knockout mice. *J. Invest. Dermatol. 115:234.*

45. Saijo, Y., M. Tanaka, M. Miki, K. Usui, T. Suzuki, M. Maemondo, X. Hong, R. Tazawa, T. Kikuchi, K. Matsushima, and T. Nukiwa. 2002. Proinflammatory cytokine IL-1β promotes tumor growth of Lewis lung carcinoma by induction of angiogenic factors: in vivo analysis of tumor-stromal interaction. *J. Immunol. 169:469.*

46. Lopez-Encuentra, A., J. L. Duque-Medina, R. Rami-Porta, A. G. de la Camara, and P. Ferrando. 2002. Staging in lung cancer: is 3 cm a prognostic threshold in pathologic stage I non-small cell lung cancer? A multicenter study of 1,020 patients. *Chest 121:1515.*

47. Glade-Bender, J., J. J. Kandel, and D. J. Yamashiro. 2003. VEGF blocking therapy in the treatment of cancer. *Exp. Opin. Biol. Ther. 3:263.*

48. Kuenen, B. C., J. Tabernero, J. Baselga, F. Cavalli, E. Pfanner, P. F. Conte, S. Seeber, S. Madhusudan, G. Deplanque, H. Huisman, et al. 2003. Efficacy and toxicity of the angiogenesis inhibitor SU5416 as a single agent in patients with advanced renal cell carcinoma, melanoma, and soft tissue sarcoma. *Clin. Cancer Res. 9:1648.*

49. Kerbel, R. S., J. Yu, J. Tran, S. Man, A. Viloria-Petit, G. Klement, B. L. Coomber, and J. Rak. 2001. Possible mechanisms of acquired resistance to anti-angiogenic drugs: implications for the use of combination therapy approaches. *Cancer Metastasis Rev. 20:79.*

50. Yu, J. L., J. W. Rak, B. L. Coomber, D. J. Hicklin, and R. S. Kerbel. 2002. Effect of p53 status on tumor response to antiangiogenic therapy. *Science 295:1526.*